

Dynamic Material Response of Graphene for FDTD Simulation of Passive Modelocking

Adam Mock

School of Engineering and Technology
Central Michigan University
Mount Pleasant MI 48859
Email: adammock1@gmail.com

Abstract—The dynamic non-linear material response of graphene is introduced into finite-difference time-domain simulations using a carrier rate equation. Experimental measurements of graphene's relaxation time and saturation intensity are used to demonstrate sub-picosecond pulse formation via passive modelocking in a 95 μm long Bragg cavity.

I. INTRODUCTION

Graphene is a two-dimensional crystalline solid consisting of a hexagonal array of carbon atoms. It exhibits a number of remarkable properties which include large electrical conductivity and high mechanical strength. Furthermore, it exhibits a nonlinear optical response by which its optical absorption decreases with increasing illumination intensity. This phenomenon is known as saturable absorption and has enabled experimental demonstration of sub-picosecond optical pulse generation in passively mode-locked fiber lasers [1], [2].

This work describes a rate equation approach for modeling the non-linear saturable absorption of graphene using the finite-difference time-domain (FDTD) method. Previous work by Bahl *et al.* utilized a similar approach that coupled the carrier density of semiconductor quantum wells to the magnitude of the electric polarization vector of the material [3]. Their method simulated short pulse generation via passive modelocking in a semiconductor Bragg cavity. In addition to the carrier rate equation, their method included a phenomenological gain/loss saturation factor $(1 + I/I_s)^{-1}$ where I_s is the saturation intensity. As pointed out in Ref [4], this phenomenological saturation factor is not needed to model gain/loss saturation as it is already accounted for in the carrier rate equation. Utilizing the carrier rate equation allows incorporation of experimental measurements of carrier relaxation rate and saturation intensity whereas the phenomenological gain/loss saturation factor $(1 + I/I_s)^{-1}$ results in an unphysical instantaneous material response. This work incorporates experimental measurements of graphene's carrier lifetime, saturation intensity and saturation depth into FDTD simulations using a carrier rate equation approach.

II. METHOD

The one-dimensional FDTD method is used for simulation of the $E_x(z)$ and $H_y(z)$ fields propagating along z . The carrier rate equation is given by

$$\frac{dN(z)}{dt} = -\frac{N(z)}{\tau} + \frac{E_x(z)J_x(z)}{\hbar\omega_0} + W_p(z) \quad (1)$$

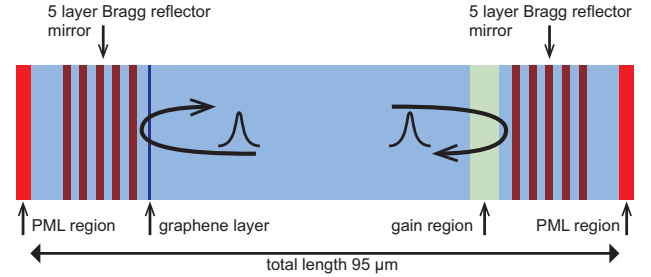


Fig. 1. Schematic diagram of Fabry-Perot Bragg cavity.

where $N(z)$ is the excited carrier density, τ is the relaxation time, $J_x(z)$ is the current density, ω_0 is the center frequency of the gain or loss spectrum, and $W_p(z)$ represents the external pump. The current density is related to the electric field via Ohm's law $J_x = \sigma(N)E_x$ where the conductivity depends linearly on carrier density via $\sigma(N) = A(N - N_0)$.

The structure analyzed using this method is depicted in Fig. 1. It consists of a Fabry-Perot cavity whose mirrors are made up of 5 layers of materials with refractive index alternating between $n = 3.5$ and $n = 1.5$ consistent with Si/SiO₂. The entire structure is 95 μm long, and the mirror reflectivity is centered at $\lambda = 1.55 \mu\text{m}$. The refractive index in the cavity region is $n = 3.5$. For the FDTD simulation $\Delta z = 19.37 \text{ nm}$, $\Delta t = 0.05167 \text{ fs}$ which is 0.8 times the Courant stability limit. Perfectly matched layer (PML) absorbing boundary conditions are used to terminate the domain. The graphene saturable absorber layer is confined to a single grid point $8\Delta z = 155 \text{ nm}$ away from the left Bragg mirror. The gain region is $150\Delta z = 2.9 \mu\text{m}$ long and is adjacent to the right Bragg mirror. The rate equation approach is used to model both the saturable absorption and saturable gain.

A. Graphene Saturable Absorption

In the graphene material, $W_p = 0$. A carrier relaxation time of $\tau = 0.1 \text{ fs}$ is used which is consistent with experimental measurements [5] although experiments with higher time resolution suggest even smaller lifetimes on the order of $\tau = 0.01 \text{ fs}$ [6]. At zero electric field, $N = 0$ and the graphene layer has an unsaturated conductivity of $-AN_0$ which is a positive number because A is set to a negative value. As the electric field impinges on the graphene layer, N increases, which reduces $\sigma(N) = A(N - N_0)$ (recalling that A is set to a negative value). Because electric conductivity

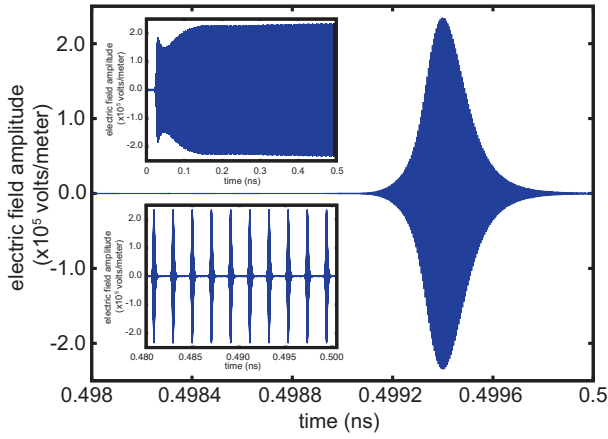


Fig. 2. E_x as a function of time over three time scales. Field was recorded to the left of the left Bragg mirror in Fig. 1.

leads to absorption, the reduction in σ with increased electric field yields saturable absorption. The unsaturated loss is set to $\pi\alpha \approx 2.3\%$ per graphene layer where α is the fine structure constant. 40 layers of graphene were used. The saturation intensity of graphene has been measured to be 0.87 MW/cm^2 and is included in the rate equation by setting $A = \hbar\omega_0/2\eta\tau I_s$ where η is the wave impedance of the medium [4]. The saturation depth was set to 30% consistent with experimental measurements.

B. Saturable Gain

Saturable gain was implemented in the same manner as saturable loss. However, W_p is varied in the range $8\text{--}30 \times 10^{33}$ carriers/sec/m³. This corresponds to an injected current density of $3.7\text{--}14 \text{ mA}/\mu\text{m}^2$ consistent with results reported in Ref [3]. The quantity N_0 is the transparency carrier density and is set to 10^{24} carriers/m³. A is set to 2×10^{-20} Siemens-m². The gain has a Lorentzian gain spectrum centered at $\lambda = 1.55 \mu\text{m}$ with a bandwidth of 60 nm.

III. RESULTS

Fig. 2 shows the electric field at the output of the left Bragg mirror as a function of time on various time scales. The simulation is initiated with a rightward directed broadband seed pulse with an amplitude at least 10^5 times smaller than the steady state field value. Simulations were run for at least 10^7 time steps and showed stability for up to 60×10^6 time steps (longer simulations were not run). Simulations were run on a single workstation. OpenMP programming was used to run four threads in parallel on a quad core Intel i7-3770K CPU.

The main plot in Fig. 2 shows a single pulse near the end of a 0.5 ns simulation. The pulse has a slightly asymmetric Lorentzian-type shape with a duration of 0.129 ps. The top inset depicts the entire time history of the field evolution. The buildup of the energy from the initial noise pulse to a steady state value is evident. The bottom inset depicts the field evolution zoomed into the time range 0.48 ns - 0.5 ns showing the repetitive pulse generation. The pulse repetition time is 2.05 ps which corresponds to the round trip time of the Fabry-Perot cavity to within 20 fs. The repetition rate is 488 GHz. The output pulse intensity is 7324 W/cm^2 .

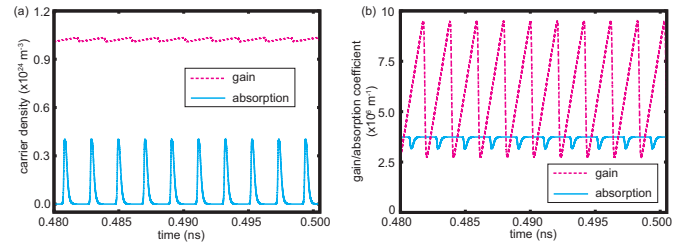


Fig. 3. (a) Time variation of the carrier density in the graphene and gain regions. (b) Time variation of the loss and gain coefficients.

Fig. 3 displays the variation in the carrier density in the gain and loss regions and the variation in the gain and loss coefficients as a function of time due to interaction with the pulsed electric field. As the optical pulse interacts with the graphene material, the absorption imparts energy to the carriers and excites them to the conduction band. Hence the carrier density goes from a nominal value of zero to $4 \times 10^{23} \text{ m}^{-3}$ at peak absorption as shown in Fig. 3(a). The two dimensional carrier density corresponding to a single graphene sheet is obtained by multiplying N by Δz divided by the number of graphene layers in Δz . This comes out to $1.94 \times 10^{14} \text{ m}^{-2}$. The gain coefficient fluctuation in Fig. 3(b) has been multiplied by 75 reflecting the longer gain region ($\times 150$) and standing wave effects ($\times 1/2$).

IV. CONCLUSION

This work presents a rate equation approach for modeling the nonlinear saturable absorption of graphene using the FDTD method. Details of the method are described, and it is applied to simulation of short pulse generation via passive mode locking. Electric field and excited carrier dynamics are presented.

ACKNOWLEDGMENT

The author would like to acknowledge funding from the Central Michigan University Office of Research and Sponsored Programs.

REFERENCES

- [1] H. Zhang, Q. Bao, D. Tang, L. Zhao, and K. Loh, "Large energy soliton erbium-doped fiber laser with a graphene-polymer composite mode locker," *Applied Physics Letters*, vol. 95, no. 14, p. 141103, 2009.
- [2] H. Kim, J. Cho, S.-Y. Jang, and Y.-W. Song, "Deformation-immunized optical deposition of graphene for ultrafast pulsed lasers," *Applied Physics Letters*, vol. 98, no. 2, p. 021104, 2011.
- [3] M. Bahl, N. C. Panoiu, and R. M. Osgood, "Modeling ultrashort field dynamics in surface emitting lasers by using finite-difference time-domain method," *Journal of Quantum Electronics*, vol. 41, no. 10, pp. 1244–1252, 2005.
- [4] F. X. Kärtner, J. Aus der Au, and U. Keller, "Mode-locking with slow and fast saturable absorbers—what's the difference?" *IEEE Journal of Selected Topics in Quantum Electronics*, vol. 4, no. 2, pp. 159–168, 1998.
- [5] R. W. Newson, J. Dean, B. Schmidt, and H. M. van Driel, "Ultrafast carrier kinetics in exfoliated graphene and thin graphite films," *Optics Express*, vol. 17, no. 4, pp. 2326–2333, 2009.
- [6] G. Xing, H. Guo, X. Zhang, T. C. Sum, C. Hon, and A. Huan, "The physics of ultrafast saturable absorption in graphene," *Optics Express*, vol. 18, no. 5, pp. 4564–4573, 2010.